Title

Paramagnetic Intermediates Generated by Radical S-Adenosylmethionine (SAM) Enzymes

Journal

Accounts of Chemical Research, 47(8)

ISSN

0001-4842

Authors

Stich, Troy A

Myers, William K

Britt, R David

Publication Date

2014-08-19

DOI

10.1021/ar400235n

Peer reviewed

ACCOUNTS of chemical research

Article

pubs.acs.org/accounts

Paramagnetic Intermediates Generated by Radical S-Adenosylmethionine (SAM) Enzymes

Troy A. Stich, William K. Myers, and R. David Britt*

Department of Chemistry, University of California, One Shields Avenue, Davis, California 95616, United States

CONSPECTUS: A $[4Fe-4S]^{+}$ cluster reduces a bound S-adenosylmethionine (SAM) molecule, cleaving it into methionine and a 5′-deoxyadenosyl radical (5′-dA•). This step initiates the varied chemistry catalyzed by each of the so-called radical SAM enzymes. The strongly oxidizing 5′-dA• is quenched by abstracting a H-atom from a target species. In some cases, this species is an exogenous molecule of substrate, for example, L-tyrosine in the [FeFe] hydrogenase maturase, HydG. In other cases, the target is a proteinaceous residue as in all the glycyl radical forming enzymes. The generation of this initial radical species and the subsequent chemistry involving downstream radical intermediates is meticulously controlled by the enzyme so as to prevent unwanted reactions. But the manner in which this control is exerted is unknown. Electron paramagnetic resonance (EPR) spectroscopy has proven to be a valuable tool used to gain insight into these mechanisms.

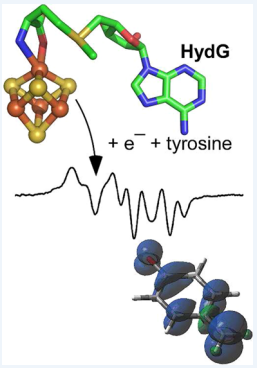

In this Account, we summarize efforts to trap such radical intermediates in radical SAM enzymes and highlight four examples in which EPR spectroscopic results have shed significant light on the corresponding mechanism. For lysine 2,3-aminomutase, nearly each possible intermediate, from an analogue of the initial 5′-dA• to the product radical L-β-lysine, has been explored. A paramagnetic intermediate observed in biotin synthase is shown to involve an auxiliary [FeS] cluster whose bridging sulfide is a co-substrate for the final step in the biosynthesis of vitamin B7. In HydG, the L-tyrosine substrate is converted in unprecedented fashion to a 4-oxidobenzyl radical on the way to generating CO and CN^{-} ligands for the [FeFe] cluster of hydrogenase. And finally, EPR has confirmed a mechanistic proposal for the antibiotic resistance protein Cfr, which methylates the unactivated sp^2-hybridized C8-carbon of an adenosine base of 23S ribosomal RNA.

These four systems provide just a brief survey of the ever-growing set of radical SAM enzymes. The diverse chemistries catalyzed by these enzymes make them an intriguing target for continuing study, and EPR spectroscopy, in particular, seems ideally placed to contribute to our understanding.

I. INTRODUCTION

An incredibly wide range of chemistries are catalyzed by the 5′-deoxyadenosyl radical (5′-dA•), which is generated by reductive cleavage of *S*-adenosyl-L-methionine (SAM) in so-called radical SAM (RS) enzymes.[1−3] SAM binds through the amine and carboxylate of the methionine moiety to the unique iron ion of a tris-cysteine liganded [4Fe−4S] cluster. The one-electron-reduced cluster transfers an electron to the sulfonium of SAM, effectively forming a new Fe−S bond[4−8] and breaking the S−5′C bond homolytically. The resultant 5′-dA• abstracts a hydrogen atom from the substrate, which is then converted to product in a manner orchestrated by the protein. Structural and kinetic characterization of the radical intermediates in these reactions is critical for obtaining atomic-level mechanistic insights.

To this end, several groups have employed electron paramagnetic resonance (EPR) spectroscopy to interrogate the radical intermediates generated after the initial H atom abstraction and prior to product formation. Excepting radicals generated by the SAM-dependent the glycyl radical enzyme (GRE) activases,[9] radical intermediates have been characterized for only 11 RS enzymes (Table 1), to the best of our knowledge. In this Account, we describe how the magnetic parameters that result from EPR spectroscopic studies of these intermediates have provided insight into the control exerted by the enzyme active site over the substrate and product radicals in order to complete the desired chemistry without deleterious side reactions.

Primary among such magnetic parameters is the molecular **g**-matrix, which is useful in assessing the gross features of unpaired spin distribution about a paramagnetic species. In the case of metal-centered radicals, the **g**-matrix is often anisotropic and reports on the metal ion oxidation state and the d-orbitals in which the unpaired electrons reside. For organic radicals, the **g**-matrix tends to be much more isotropic, but coupling of the unpaired spin with nearby magnetic nuclei (^{1}H, ^{2}H, ^{13}C, ^{14}N, ^{15}N, etc.) can lead to resolvable structure in the EPR signal (see Figures 1, 6, and 8A, for example). More often, however, this hyperfine interaction (HFI)-induced splitting tends to be obscured in the inhomogeneously broadened EPR line. Advanced EPR methods[10] including electron−nuclear double resonance (ENDOR, see Figures 2 and 8) and electron spin−echo envelope modulation (ESEEM, see Figures 4 and 5) techniques can resolve these interactions. The resultant HFI tensor is composed of isotropic (A_{iso}) and anisotropic components. A_{iso} arises from unpaired spin at the magnetic

Received: October 7, 2013
Published: July 3, 2014

   dx.doi.org/10.1021/ar400235n | *Acc. Chem. Res.* 2014, 47, 2235−2243

Table 1. Intermediates of Radical SAM Enzymes Probed Using EPR[a]

enzyme	substrate	observed intermediate	refs
BioB	DTB	DTB-[2Fe−2S]$^+$	12−14
BtrN	DOIA	DOIA$^\bullet$	15
		auxiliary [4Fe−4S]$^+$	16
Cfr	155-mer RNA	adenine linked *m*-Cys355	17
DesII	TDP-D-quinovose	C3 α-hydroxyalkyl$^\bullet$	18
GAM	glutamate	glutamate-PLP$^\bullet$	19
HemN	corproporhyrinogen III	H atom off propionate	20
HydG	L-tyrosine	4OB$^\bullet$	21
LAM	lysine	lysine-PLP$^\bullet$	22
NirJ	precorrin-2	unknown	23
NocL	L-tryptophan	L-tryptophan$^\bullet$	24
ThiC	none	peptide-backbone$^\bullet$	25

[a]Abbreviations: 4OB = 4-oxidobenzyl; BioB = biotin synthase; BtrN = DOIA dehydrogenase; Cfr = SAM:A2503 23S RNA methyltransferase; DesII = TDP-4-amino-4,6-dideoxy-D-glucose deaminase; DOIA = 2-deoxy-*scyllo*-inosamine; DTB = dethiobiotin; GAM (EAM) = glutamate 2,3-aminomutase; HemN = coproporphyrinogen III oxidase; HydG = [FeFe] hydrogenase maturase; LAM (KAM) = lysine 2,3-aminomutase; NirJ = involved in heme d_1 biosynthesis; NocL = 3-methyl-2-indolic acid synthase; PLP = pyridoxal-5′-phosphate; TDP = thymidine diphosphate; ThiC = 4-amino-5-hydroxymethyl-2-methylpryimidine phosphate synthase.

nucleus, achieved via direct overlap of this nucleus with an orbital containing the unpaired electron, and from spin polarization of the s-orbital electrons by the valence shell. The anisotropic portion results from a combination of a through-space dipolar interaction (**T**) and any asymmetric spin density distribution among orbitals centered on the magnetic nucleus. If anisotropy in the **g**-matrix can be ignored, the centers containing the unpaired electron spin and magnetic nucleus are rather distant from one another (r > 2.5 Å), and orbital contributions to the HFI are small (estimates for this orbital contribution to the HFI anisotropy can be made from the magnitude of the A_{iso}; see ref 11 for a relevant application of this method), the elements of **T** reduce to

$$\mathbf{T} = \frac{\mu_0}{4\pi\hbar} g_e \mu_B g_N \mu_N \rho \left(\frac{3\cos^2\theta - 1}{r^3} \right) \quad (1)$$

The electron and nuclear **g**-factors are given by g_e and g_N, respectively; μ_B and μ_N are the Bohr and nuclear magnetons, respectively. The spatial separation between the electron and nuclear spin is represented by r, and the angle of this vector with respect to applied magnetic field is defined as θ. The unpaired spin population on the central ion is given by ρ. In this long interspin distance limit, **T** = [$-T$, $-T$, +2T], where T is proportional to the inverse of the cube of the distance between the electron and nuclear spins. Thus, with knowledge of these magnetic parameters, an exquisitely detailed structural picture of these intermediates can be drawn.

Paramagnetic RS intermediates have been observed under steady-state conditions in reactions of lysine 2,3-aminomutase (LAM)[22] and glutamate 2,3-aminomutase (GAM).[19] We discuss the chemical nature of this LAM-generated radical in section II, along with those of other paramagnetic species trapped using lysine and SAM analogues. Paramagnetic intermediates have also been caught by freeze-quenching the reaction mixture (enzyme, SAM, substrate, and reductant) under pre-steady-state conditions: notably for 2-deoxy-*scyllo*-inosamine dehydrogenase (BtrN),[15] the methyltransferase Cfr,[17] biotin synthase (BioB),[13,26] and the hydrogenase maturation enzyme HydG.[21] BtrN, BioB, and HydG are members of a growing subclass of RS enzymes that possess one or more [FeS] clusters in addition to the [4Fe−4S] cluster that binds and cleaves SAM.[27] We present recent EPR spectroscopic findings concerning radical intermediates in the BioB- and HydG-catalyzed reactions in sections III and IV, respectively. In section V, we highlight a recent effort to trap the RNA-based radical intermediate in the methylation reaction catalyzed by Cfr.[17] Cfr and the similar RlmN are founding members of the class of RS-mediated methyltransferases.[28]

The systems described in this Account represent only a small subset of the many diverse RS enzymes that exist. Because the 5′-dA$^\bullet$ generates paramagnetic intermediates, we expect EPR spectroscopy to continue to be a critical tool in further exploration of RS enzymology.

II. LYSINE 2,3-AMINOMUTASE

Paramagnetic intermediates and analogues of intermediates of the LAM catalytic cycle have been generated at essentially every step of the isomerization of L-α-lysine to L-β-lysine (Figure 1). The holoenzyme coordinates a PLP cofactor through formation of an internal aldimine with Lys337. As L-α-lysine binds, PLP forms an external aldimine linkage to the α-amine group of the substrate. Reductive cleavage of SAM leads to formation of 5′-dA$^\bullet$ that is too fleeting to be observed. However, substitution of SAM with *S*-3′,4′-anhydroadenosyl-L-methionine leads to generation of a stable allylic analogue of 5′-dA$^\bullet$.[29] Deuterium labeling at positions 2′, 3′, and 5′ dramatically alters the continuous-wave (CW) EPR spectrum (cf. Figure 1A,B) as the ^{1}H HFIs are reduced by a factor of 6.51 (the ratio of the ^{1}H to ^{2}H nuclear g-values, g_N). This behavior upon isotope substitution confirms the assignment of this signal to an anhydroadenosyl π-radical in which the unpaired electron is delocalized equally over carbons 3′ and 5′.[30] The magnitude of A_{iso} for the proton bound to C2′ is sensitive to the orientation of the C2′—H bond with respect to the spin-carrying C3′-2p$_z$ orbital.[30] This angle was found to be 37° and affords a picture of coenzyme cleavage products immediately after C−S bond scission.

When using SAM, the posthomolysis 5′-dA$^\bullet$ abstracts the *pro*-R H atom from the β-carbon of lysine but converts rapidly to the product radical (see below).[32] To observe a substrate-like radical again requires trickery: using either *trans*-4,5-dehydro-L-lysine (*an*Lys)[33] or 4-thia-L-lysine (4-thia-Lys) halts the mutase reaction in a state that resembles L-α-lysine$^\bullet$.

With 4-thia-Lys (Figure 1C), the resultant radical is localized in the 2p$_z$ orbital of the β-carbon of the substrate and is thus a high-fidelity model of the α-lysine radical generated immediately following H atom abstraction by 5′-dA$^\bullet$. ENDOR spectra of 4-thia-Lys$^\bullet$ yielded full hyperfine tensors for the interaction between the substrate radical and both the ^{13}C-labeled 5′-carbon (I = 1/2) of 5′-dAH and the thiomethyl-carbon of methionine (Figure 2).[11] ENDOR doublets ascribed to ^{13}C nuclei are identified based on their being split symmetrically by the magnitude of the HFI about the ^{13}C Larmor frequency ($\nu_L{}^{13}$C, determined using g_N), or in the case of very strong coupling, the doublet will be centered at a frequency equal to half the HFI and split by twice the Larmor frequency. Strong couplings are more easily observed using Davies ENDOR, whereas weaker ones can be resolved using Mims ENDOR or

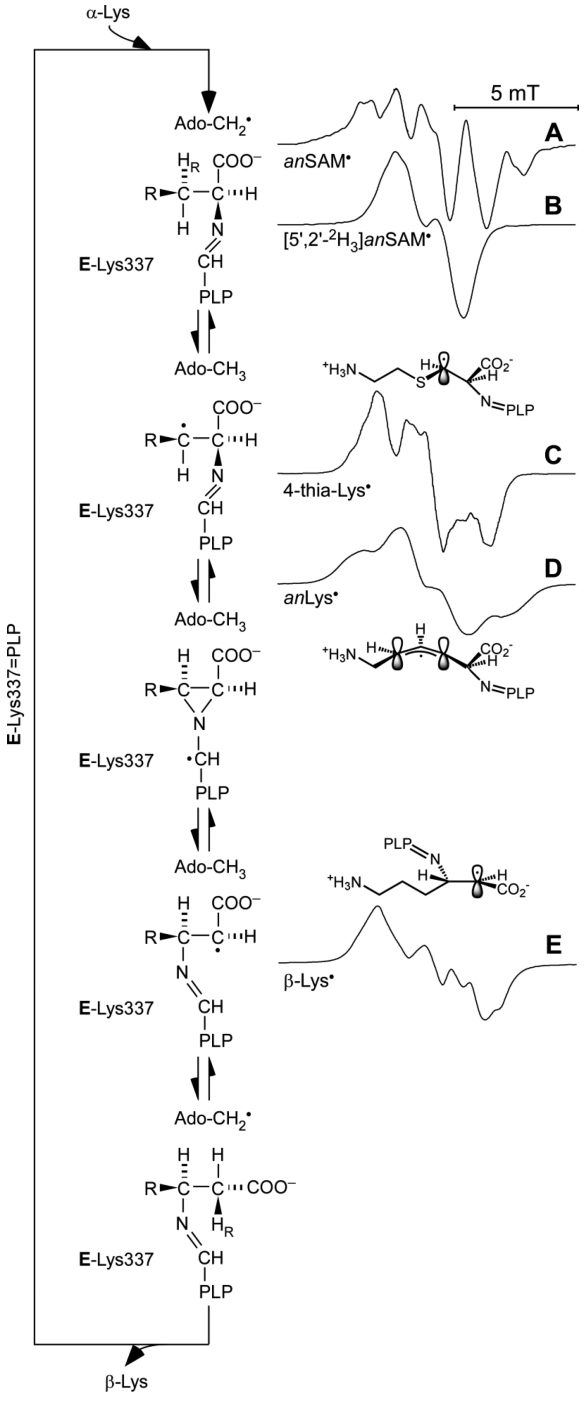

Figure 1. Reaction cycle for LAM with corresponding X-band (9 GHz) CW EPR spectra of intermediates or analogues of intermediates. Adapted from ref 31.

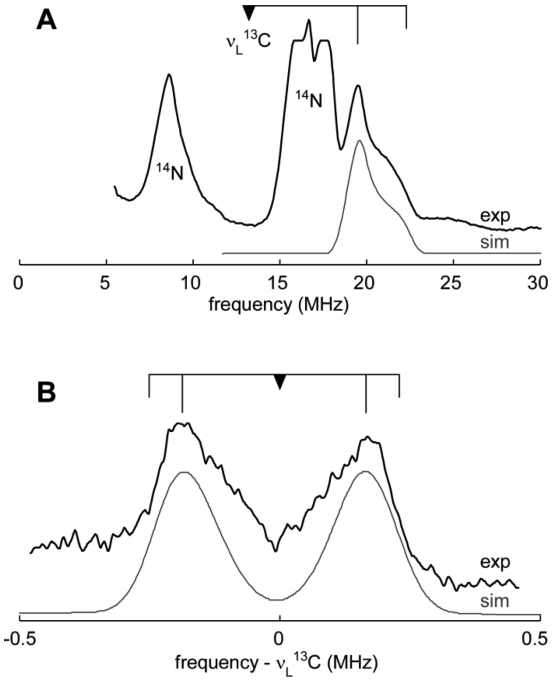

Figure 2. Q-band ^{13}C ENDOR of dithionite-reduced LAM reacted with 4-thia-Lys and SAM labeled at the 5′-carbon (A) or the *S*-methyl carbon (B). Adapted from ref 11.

ESEEM spectroscopies.[10] Hyperfine anisotropy is evident in the spectra presented in Figure 2, with the perpendicular turning point appearing to be twice as intense as the parallel turning point. Using eq 1, analysis of the two ^{13}C HFIs determined from the ENDOR data in Figure 2 (A(5′-^{13}C-dAH) = [15.2, 15.2, 17.7] MHz and A(*methyl*-^{13}C methionine) = [0.4, 0.4, 0.7] MHz) revealed that the β-carbon of 4-thia-Lys$^{\bullet}$ is ≥4.1 Å distant from the methionine methyl carbon and is in van der Waals contact with the 5′-carbon of 5′-dAH.[11] A similar analysis of the corresponding ^{31}P HFI indicated that the phosphate phosphorus of PLP is just 4.3 Å from the lysine β-carbon whereas an internuclear distance of ∼7 Å was found in the X-ray structure of the oxidized form of the enzyme.[34] This finding points to a rather dramatic movement of PLP during the initial stages of the reaction.

These distances change slightly when using *an*Lys, which affords an allylic radical wherein the unpaired spin is shared by the β and δ carbons of the lysine analogue (Figure 1D).[33] Again, analysis of the dipolar part of the ^{13}C HFI shows that the mean distance to the methionine methyl group lengthens to 5.5 Å and shrinks to 3.6 Å for the radical−P distance. However, the 5′ methyl group of 5′-dAH remains in close proximity to the substrate radical.

The native (as yet unobserved) substrate radical is thought to rapidly convert through an azacyclopropylcarbinyl radical intermediate to a "product"-radical centered on the α-carbon of lysine with the PLP-bound amino group shifted to the β-carbon. This α-carbon radical has been observed under steady-state conditions (excess of substrate).[22] EPR spectra of this intermediate obtained using site-specific isotopically labeled lysine as substrate confirmed the assignment of this species to L-β-lysine$^{\bullet}$.[35] ^{13}C ENDOR again showed a close association between L-β-lysine$^{\bullet}$ and the 5′-methyl group of 5′-dAH. That this close proximity of 5′-dAH to the substrate/product radical is maintained throughout the reaction cycle is thought to minimize the potential for unwanted side reactions of the reactive intermediates and help to recycle SAM for the next turnover. ESEEM results show that the PLP cofactor plays an important role in stabilizing this species by delocalizing the unpaired electron onto the π-system of its pyridine ring yielding N^3-(5′-phosphopyridoxylidene)-β-lysin-2-yl.[36,37]

III. BIOTIN SYNTHASE

For BioB, a $(Cys)_3$Arg-coordinated [2Fe−2S] cluster is employed as a cosubstrate, and one of the bridging sulfides is transferred to dethiobiotin (DTB) to complete the thiophane

dx.doi.org/10.1021/ar400235n | Acc. Chem. Res. 2014, 47, 2235−2243

ring as the final step in the biosynthesis of vitamin B_7 (Figure 3, top).[38] The X-ray crystal structure of BioB with SAM and DTB

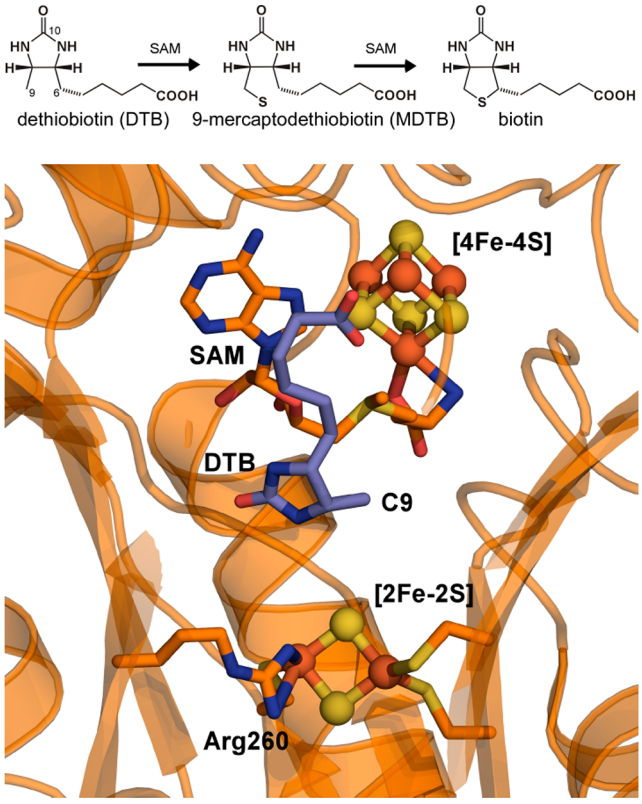

Figure 3. Overall BioB-catalyzed reaction (top) and active site structure of BioB with SAM and DTB bound (bottom, PDB accession code 1R30).

bound shows the SAM molecule coordinating to the [4Fe−4S] via the amine and carboxylate moieties (Figure 3, bottom).[39] In this geometry, the 5′-C of SAM is situated 3.8 Å from C9 of DTB, the target of the first H atom abstraction by 5′-dA•. C9 is 4.6 Å away from the nearer sulfide of the [2Fe−2S] cosubstrate. Thus, to attack the bridging sulfide, a significant geometric rearrangement of DTB• within the enzyme active site is required. Since DTB is held in place primarily through hydrogen bonds between the DTB imidazolidinone and Asn151, Asn153, and Asn222, this attack could be accomplished through a simple hinge motion around these bonds.[40]

H atom abstraction at the C9 position of DTB (Figure 3, top) leads to formation of a catalytically competent species with an EPR spectrum consistent with a reduced [2Fe−2S] cluster.[13,26] The identity of this paramagnetic species was probed further using hyperfine sublevel correlation spectroscopy (HYSCORE), a two-dimensional ESEEM technique. HYSCORE spectroscopy is useful in untangling resonances from multiple hyperfine-coupled nuclei, which would be overlapping in one-dimensional results. Comparing the HYSCORE spectrum of the intermediate generated using natural-abundance wild-type enzyme to that made using BioB that was enriched with *guanidino*-$^{15}N_2$−Arg allowed us to confirm that the paramagnetic species arises from the reduced form of the arginine-coordinated [2Fe−2S] (Figure 4). All features in the ^{14}N-Arg HYSCORE spectrum were altered upon this ^{15}N-isotopic substitution, and the resulting two sets of cross-peaks correspond to the two guanidino nitrogens of

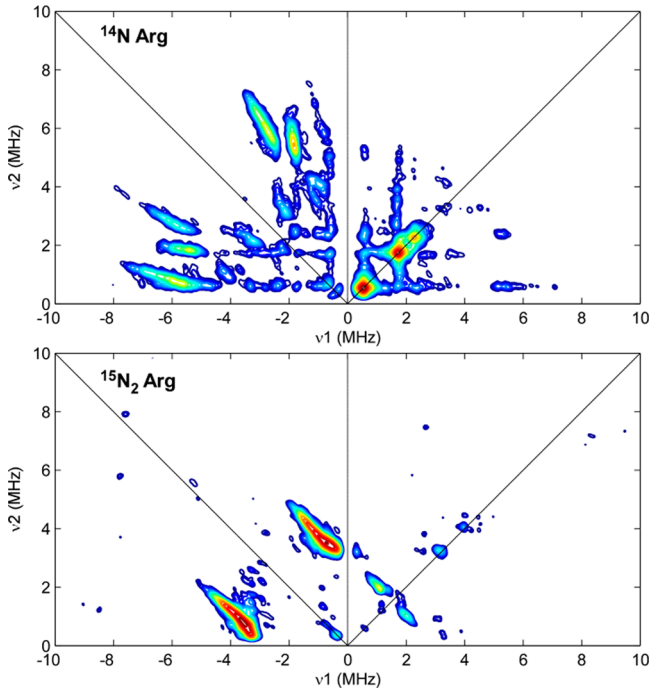

Figure 4. X-band HYSCORE spectra of the BioB paramagnetic intermediate produced in BioB purified from *Escherichia coli* grown with natural abundance arginine (top) and (*guanidino*-$^{15}N_2$)-L-arginine (bottom). Adapted from ref 14.

Arg260. Orientation-selected HYSCORE results (wherein the HYSCORE spectrum is collected at resonant magnetic field positions across the EPR envelope) provided the complete hyperfine tensor for each ^{15}N nucleus. Using a distributed point-dipole model for exchange-coupled clusters,[41,42] we analyzed the anisotropic part of the tensor to determine the likely position of the nitrogen atoms in relation to the two Fe ions whose positions were fixed based on the crystal structure coordinates of oxidized BioB. The Fe−N internuclear distances predicted by this method are in close agreement with those determined from the crystal structure of the holo-form in the presence of substrate but before reduction.

The HYSCORE spectrum of the paramagnetic intermediate generated using natural-abundance BioB and (*9-methyl*-^{13}C)-DTB displays new correlation ridges that have no counterpart in the corresponding natural-abundance DTB spectrum (Figure 5). These features correspond to an axial ^{13}C HFI of [1.2, 1.2, 5.7] MHz. The relatively large isotropic contribution to the hyperfine tensor (A_{iso} = 2.7 MHz) is similar to that found for the β-C of cysteine ligands to the Fe(II,III) form of ferredoxin.[43] That the anisotropic ^{13}C HFI contribution is also relatively large (T = 1.5 MHz) corroborates the close association of C9 with the [2Fe−2S] cluster. Thus, we propose that a mercaptodethiobiotin (MDTB) intermediate is formed as a ligand to the remnants of the [2Fe−2S] (Figure 5C).

Having the radical character of the MDTB intermediate essentially carried by the [2Fe−2S] rather than a terminal sulfur denudes the reactivity of the MDTB moiety allowing the second H atom abstraction to occur in due course. Thus, the [2Fe−2S] also facilitates inner-sphere one-electron oxidation of the sulfide concurrent with formation of the new C−S bond and provides a rapid and safe means for quenching the radical at the end of each step initiated by SAM homolysis.[40]

dx.doi.org/10.1021/ar400235n | *Acc. Chem. Res.* 2014, 47, 2235−2243

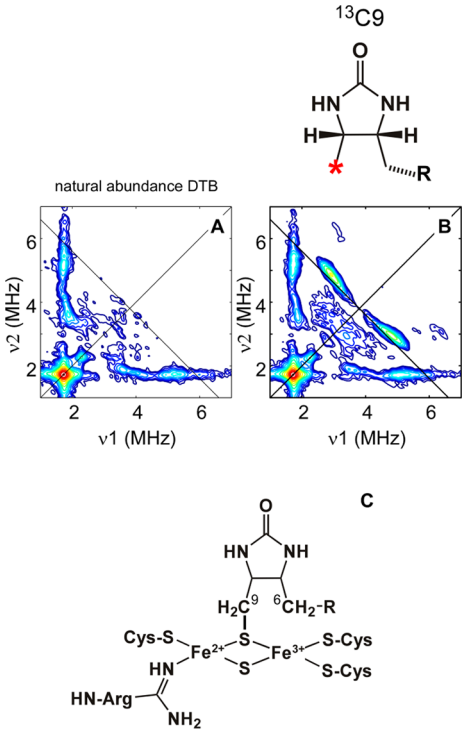

Figure 5. X-band HYSCORE spectra of the BioB paramagnetic intermediate prepared with (A) natural abundance DTB and (B) (*9-methyl*-^{13}C)-DTB. Adapted from ref 14. The proposed structure of the intermediate is shown in panel C.

IV. HydG INVOLVEMENT IN HYDROGENASE MATURATION

The enzymatic machinery for biosynthesis of the H-cluster (a dinuclear Fe(CO)(CN) complex bridged by azadithiolate and linked via cysteine to a [4Fe−4S] cluster) of [FeFe] hydrogenases includes gene products HydEFG. Both HydE and HydG are RS enzymes. Results from biochemical and spectroscopic studies have shown unequivocally that L-tyrosine is the substrate of HydG and that the atoms of the amino acid backbone are incorporated into all five CO and CN^- ligands to the H-cluster[44−46] with *p*-cresol produced as a byproduct.[47]

In addition to the SAM-binding [4Fe−4S], HydG employs an auxiliary [FeS] that is believed to be coordinated by three cysteine residues located in the C-terminal domain. The role of this second cluster is currently unclear, but it may assist in activating tyrosine for $C_\alpha-C_\beta$ bond homolysis. Interestingly, a number of other RS $C_\alpha-C_\beta$ lyases also employ a second cluster,[48] but not all.[24,49]

Proposed mechanisms for the HydG reaction begin with H atom abstraction from the phenolic group of tyrosine by the 5′-dA$^\bullet$. At this point, the neutral tyrosine radical could fragment heterolytically or homolytically at the C_α—C_β bond, yielding either a 4-oxidobenzyl anion radical (4OB$^\bullet$) and dehydroglycine (DHG) or 4-methylidenecyclohexa-2,5-dien-1-one and a glycyl radical, respectively. Freeze-quenching the reaction of reduced HydG+SAM with L-tyrosine a few seconds after mixing leads to a strong signal centered at $g = 2$ likely arising from an organic radical.[21] This radical disappears as new Fe-bound CO and CN species appear.[50]

Using a variety of specifically isotope-labeled tyrosines as substrate, we have been able to rigorously determine the molecular origin of the RFQ-trapped radical. The Q-band CW EPR spectrum (Figure 6) of the cryo-trapped radical obtained using natural abundance tyrosine (a) is unaltered by ^{13}C-

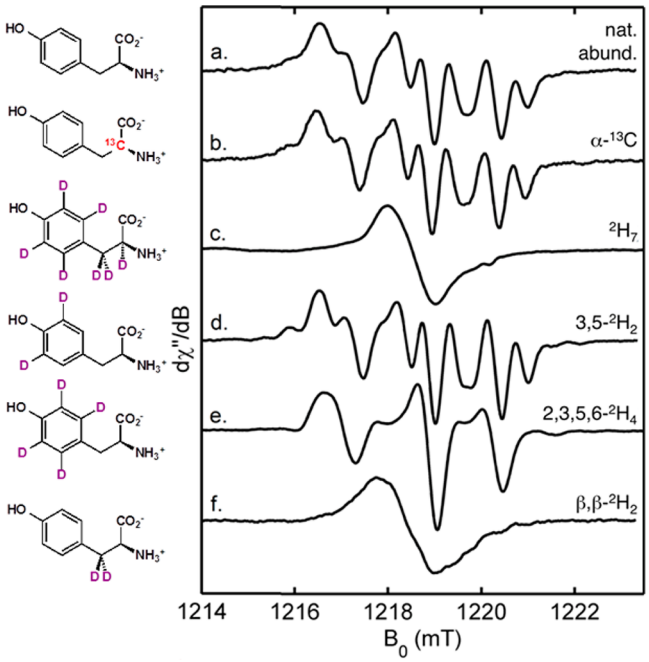

Figure 6. Q-band CW EPR spectra (right) of the freeze-quenched radical generated by reacting dithionite-reduced HydG with SAM and one of a set of isotopically labeled tyrosines (left). Adapted from ref 21.

labeling at the α-C (b), proving that the radical species does not correspond to the proposed glycyl intermediate.[51] In contrast, the line shape collapses when the radical is generated using $^2H_7$-tyrosine (c), a signature that has been used to assign protein radicals to tyrosine-derived species.[52] For neutral tyrosine radicals, there is appreciable spin density on the oxygen and on the 1-, 3-, and 5-carbons of the ring, and the 1-C transfers angular-dependent inequivalent couplings to the two protons bound to the β-C. The remaining spectra presented in Figure 6 show that the trapped species is something altogether different. The spectrum of the 3,5-$^2H_2$ tyrosine sample (d) is almost identical to that of the natural-abundance tyrosine (a), whereas the addition of two deuterons at positions 2 and 6 (e) causes a dramatic change, showing that the ring electron spin density has shifted to the 2,6-C's at the expense of the 3,5-C's. The remaining hyperfine coupling is to the two β-C protons, which shows a 1:2:1 pattern diagnostic of two equivalently coupled protons. When these are instead deuterated (f), this 1:2:1 pattern is eliminated, and we see the largest effect of all the labels, showing the greatest spin density is on the β-C. Results from DFT calculations support the assignment of this radical to the cleaved tyrosine fragment to 4OB$^\bullet$, which is the precursor to *p*-cresol.

To what degree the secondary [FeS] is involved is a key question for this enzyme and all others that employ such auxiliary clusters. Interestingly, in the case of MoaA, a participant in the molybdenum cofactor biosynthetic pathway, the auxiliary cluster was shown by X-ray crystallography[53] and ENDOR spectroscopy[54] to bind the substrate guanosine 5′-triphosphate (5′-GTP) directly. This led us to propose that in HydG a tyrosine-derived fragment (perhaps DHG) could bind to the unique iron of the three-cysteine-coordinated cluster

dx.doi.org/10.1021/ar400235n | Acc. Chem. Res. 2014, 47, 2235−2243

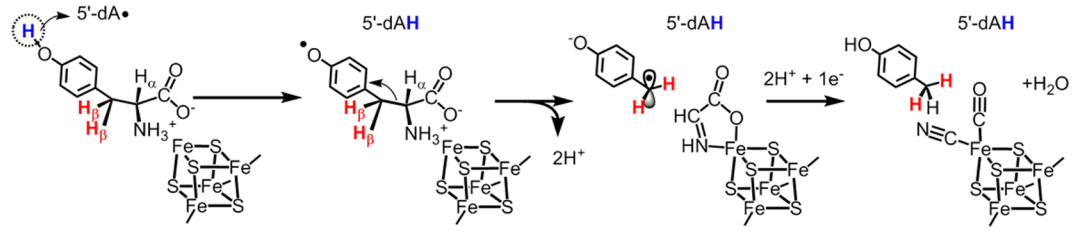

Figure 7. Proposed mechanism for tyrosine fragmentation to CO and CN^- ligands by HydG for H-cluster biosynthesis.

housed in the C-terminus (see Figure 7). Once 4OB• is generated in HydG, it requires a H atom to convert to the *p*-cresol product. It is attractive to think that this H atom comes from the putative [FeS]-bound DHG and the resultant DHG radical leads to the formation of CO and CN^-. Using Fourier-transform infrared spectroscopy, we have shown that these tyrosine-derived diatomic ligands bind to a single Fe center in HydG.[50] By selectively labeling HydG with ^{57}Fe and monitoring the reaction using ENDOR spectroscopy, we showed that iron from HydG is subsequently incorporated into the [2Fe] part of the H-cluster of mature hydrogenase with its cargo of diatomic ligands presumably intact.[50]

V. RNA METHYLATION

Two RS enzymes, Cfr and RlmN, catalyze the methylation of unactivated sp^2-hybridized C atoms on adenosine 2503 (at C8 and C2, respectively) of 23S rRNA.[55] A methyl group is first transferred from one molecule of SAM to a conserved cysteine side chain.[56] The X-ray structure of RlmN with SAM shows that Cys355 is already methylated and in position for reaction with 5′-dA• produced when a second SAM molecule coordinates the RS [FeS] and is reductively cleaved.[56] The 5′-dA• abstracts a H atom from the nascent *S*-methyl group, which then attacks the C8 (or C2), forming a covalent bond between the methylated cysteine and the adenosine base. This radical adduct has recently been trapped by freeze-quenching of the reaction of Cfr with a 155-mer RNA substrate analogue.[17] The corresponding EPR spectrum is reminiscent of that measured for γ-irradiated DNA and is sensitive to perdeutero-labeling of the adenosine in the substrate (Figure 8A). ENDOR spectra (Figure 8B–D) identify five protons with hyperfine couplings ranging from 2–30 MHz. The most-strongly coupled proton with HFI = [80, 82, 85] MHz (the corresponding deuterium coupling is designated D_1 centered at 6.2 MHz in Figure 8B and is related to the proton coupling by the ratio of the respective Larmor frequencies) is bound to C8. That the HFI is very isotropic points to the conversion of C8 from sp^2 to sp^3. Protons coupled to sp^2 π-radicals tend to have axial, not isotropic, HFI due to the asymmetric interaction with the unpaired spin density in the adjacent carbon $2p_z$-based orbital. Most illuminating, reaction of the enzyme with ^{13}C-methyl-SAM dramatically alters the spectrum and confirms the identity of this intermediate as an adenine-centered radical that is covalently attached at C8 to the *S*-(^{13}C)methylated Cys355.

VI. SUMMARY AND OUTLOOK

Based on a key bioinformatics study, nearly 50 000 RS enzymes have been identified.[57,58] However, functions of only approximately 60 have been elucidated. Due to the important and exotic chemistries catalyzed by RS enzymes, further investigation into atomic-level details of their mechanisms is clearly warranted. The first step of the reaction is common to

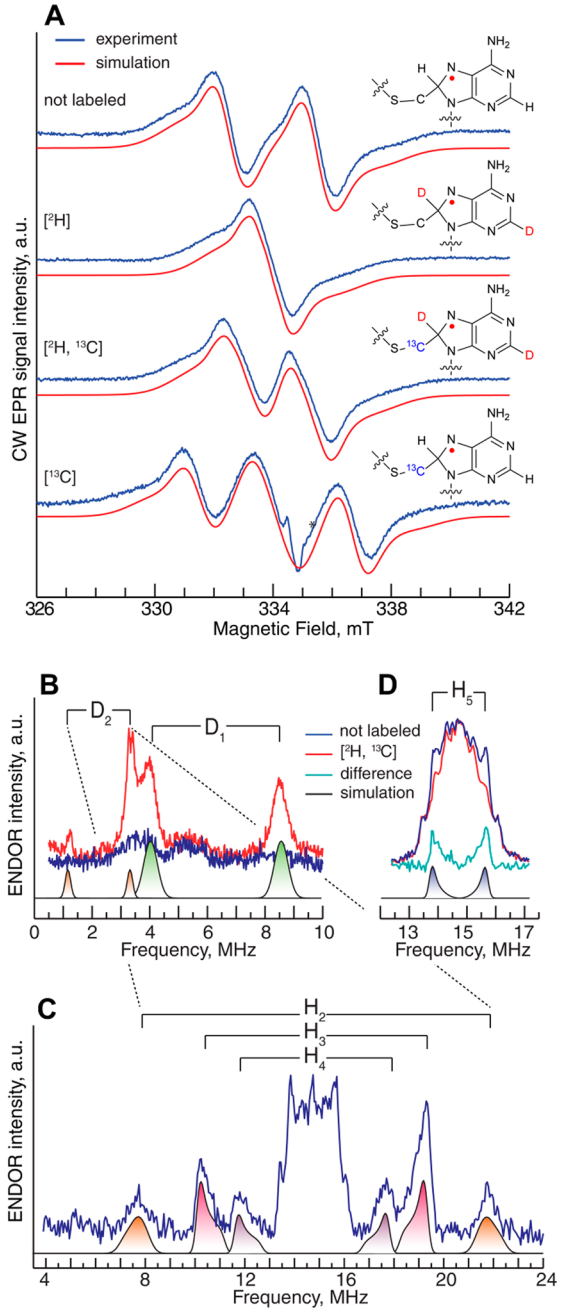

Figure 8. X-band CW EPR (A) and ENDOR (B–D) spectroscopic characterization of the organic radical intermediate in reaction of Cfr with 155-mer RNA. Adapted from ref 17.

almost all RS enzymes, namely, the formation via reductive cleavage of a 5′-dA• that abstracts a H atom from the substrate. However, 5′-dA• is so reactive that it has yet to be observed

dx.doi.org/10.1021/ar400235n | *Acc. Chem. Res.* 2014, 47, 2235–2243

natively. DFT results indicate that H-bonds to the adenosyl moiety play a crucial role in guiding this radical to the desired target;[59] there is significant structural homology around the SAM-binding site suggesting that this porting mechanism, whatever it may be, is largely conserved.[60]

It is the next stage of the RS mechanism, the subsequent reaction of the substrate radical to form product, that is likely unique for each enzyme and the target of research effort described above. In the case of LAM, EPR studies on radical intermediates of the reaction have revealed that the PLP cofactor traverses a large distance within the active site over the course of the reaction while the lysine substrate remains close to the deoxyadenosine homolysis product. HYSCORE spectroscopic results on the paramagnetic intermediate generated during biotin biosynthesis show that the substrate DTB moves several angstroms after H atom abstraction at C9 in order to attack the bridging sulfide of the [2Fe−2S]. These spectroscopically determined structural constraints have been invaluable in filtering mechanistic proposals. As such, EPR spectroscopy is expected to continue being an important tool in RS enzyme research.

AUTHOR INFORMATION

Corresponding Author

*E-mail: rdbritt@ucdavis.edu.

Notes

The authors declare no competing financial interest.

Biographies

Troy A. Stich received his B.S. in Chemistry in 2000 from Carnegie Mellon University working with Prof. Michael P. Hendrich. In 2005, he obtained his Ph.D. in Physical Chemistry at the University of Wisconsin, Madison, working with Prof. Thomas C. Brunold on the biosynthesis of coenzyme B_{12}. He is currently an Associate Research Specialist with Prof. R. David Britt.

William K. Myers received his B.A. in Chemistry in 2003 from Carleton College after a year of studying under Dr. Mary P. Neu at Los Alamos National Laboratory. In 2008, he obtained a Ph.D. in Inorganic Chemistry from the University of New Mexico under Prof. David L. Tierney, on the NMR and EPR of high-spin Co(II) in metalloenzymes. Following postdoctoral scholarships with Prof. Charles P. Scholes in SUNY-Albany and Prof. R. David Britt, he is now the Scientific Applications Manager at CAESR, University of Oxford.

R. David Britt received his B.S. in physics at North Carolina State University. He received his Ph.D. in physics at U.C. Berkeley in 1988 under Prof. Melvin P. Klein and has been at U.C. Davis since then.

ACKNOWLEDGMENTS

We are grateful for funding from the National Institutes of Health (Grant GM104543) and from the Division of Chemical Sciences, Geosciences, and Biosciences (Grant DE-FG02-11ER16282) of the Office of Basic Energy Sciences of the United States Department of Energy. We are indebted to our collaborators Professors Joseph P. Jarrett (University of Hawai'i) and James R. Swartz (Stanford University) and their students Corey J. Fugate and Jon M. Kuchenreuther for supplying the samples used in the studies of BioB and HydG, respectively. We also thank Daniel Suess for helpful discussions and Alexey Silakov, Tyler Grove, and Prof. Squire Booker (Pennsylvania State University) for supplying figures on Cfr.

REFERENCES

(1) Frey, P. A.; Hegeman, A. D.; Ruzicka, F. J. The radical SAM superfamily. *Crit. Rev. Biochem. Mol. Biol.* **2008**, *43*, 63−88.

(2) Broderick, J. B.; Duffus, B. R.; Duschene, K. S.; Shepard, E. M. Radical S-adenosylmethionine enzymes. *Chem. Rev.* **2014**, *114*, 4229−4317.

(3) Vey, J. L.; Drennan, C. L. Structural insights into radical generation by the radical SAM superfamily. *Chem. Rev.* **2011**, *111*, 2487−2506.

(4) Cosper, N. J.; Booker, S. J.; Ruzicka, F.; Frey, P. A.; Scott, R. A. Direct FeS cluster involvement in generation of a radical in lysine 2,3-aminomutase. *Biochemistry* **2000**, *39*, 15668−15673.

(5) Chen, D.; Walsby, C.; Hoffman, B. M.; Frey, P. A. Coordination and mechanism of reversible cleavage of S-adenosylmethionine by the [4Fe-4S] center in lysine 2,3-aminomutase. *J. Am. Chem. Soc.* **2003**, *125*, 11788−11789.

(6) Nicolet, Y.; Amara, P.; Mouesca, J.-M.; Fontecilla-Camps, J. C. Unexpected electron transfer mechanism upon AdoMet cleavage in radical SAM proteins. *Proc. Natl. Acad. Sci. U.S.A.* **2009**, *106*, 14867−14871.

(7) Kampmeier, J. A. Regioselectivity in the homolytic cleavage of *S*-adenosylmethionine. *Biochemistry* **2010**, *49*, 10770−10772.

(8) Dey, A.; Peng, Y.; Broderick, W. E.; Hedman, B.; Hodgson, K. O.; Broderick, J. B.; Solomon, E. I. S K-edge XAS and DFT calculations on SAM dependent pyruvate formate-lyase activating enzyme: Nature of interaction between the Fe4S4 cluster and SAM and its role in reactivity. *J. Am. Chem. Soc.* **2011**, *133*, 18656−18662.

(9) Shisler, K. A.; Broderick, J. B. Glycyl radical activating enzymes: Structure, mechanism, and substrate interactions. *Arch. Biochem. Biophys.* **2014**, *546*, 64−71.

(10) Schweiger, A.; Jeschke, G. *Principles of Pulse Electron Paramagnetic Resonance*; Oxford University Press: Oxford, U.K.; New York, 2001.

(11) Lees, N. S.; Chen, D.; Walsby, C. J.; Behshad, E.; Frey, P. A.; Hoffman, B. M. How an enzyme tames reactive intermediates: Positioning of the active-site components of lysine 2,3-aminomutase during enzymatic turnover as determined by ENDOR spectroscopy. *J. Am. Chem. Soc.* **2006**, *128*, 10145−10154.

(12) Jameson, G. N. L.; Cosper, M. M.; Hernandez, H. L.; Johnson, M. K.; Huynh, B. H. Role of the 2Fe-2S cluster in recombinant *Escherichia coli* biotin synthase. *Biochemistry* **2004**, *43*, 2022−2031.

(13) Taylor, A. M.; Stoll, S.; Britt, R. D.; Jarrett, J. T. Reduction of the 2Fe-2S cluster accompanies formation of the intermediate 9-mercaptodethiobiotin in *Escherichia coli* biotin synthase. *Biochemistry* **2011**, *50*, 7953−7963.

(14) Fugate, C. J.; Stich, T. A.; Kim, E. G.; Myers, W. K.; Britt, D.; Jarrett, J. T. 9-Mercaptodethiobiotin is generated as a ligand to the 2Fe-2S^{+} cluster during the reaction catalyzed by biotin synthase from *Escherichia coli*. *J. Am. Chem. Soc.* **2012**, *134*, 9042−9045.

(15) Yokoyama, K.; Ohmori, D.; Kudo, F.; Eguchi, T. Mechanistic study on the reaction of a radical SAM dehydrogenase BtrN by electron paramagnetic resonance spectroscopy. *Biochemistry* **2008**, *47*, 8950−8960.

(16) Grove, T. L.; Ahlum, J. H.; Sharma, P.; Krebs, C.; Booker, S. J. A consensus mechanism for radical SAM-dependent dehydrogenation? BtrN contains two 4Fe-4S clusters. *Biochemistry* **2010**, *49*, 3783−3785.

(17) Grove, T. L.; Livada, J.; Schwalm, E. L.; Green, M. T.; Booker, S. J.; Silakov, A. A substrate radical intermediate in catalysis by the antibiotic resistance protein Cfr. *Nat. Chem. Biol.* **2013**, *9*, 422−427.

(18) Ruszczycky, M. W.; Choi, S.-h.; Mansoorabadi, S. O.; Liu, H.-w. Mechanistic studies of the radical *S*-adenosyl-L-methionine enzyme DesII: EPR characterization of a radical intermediate generated during its catalyzed dehydrogenation of TDP-D-quinovose. *J. Am. Chem. Soc.* **2011**, *133*, 7292−7295.

(19) Ruzicka, F. J.; Frey, P. A. Glutamate 2,3-aminomutase: A new member of the radical SAM superfamily of enzymes. *Biochim. Biophys. Acta* **2007**, *1774*, 286−296.

(20) Layer, G.; Pierik, A. J.; Trost, M.; Rigby, S. E.; Leech, H. K.; Grage, K.; Breckau, D.; Astner, I.; Jansch, L.; Heathcote, P.; Warren,

M. J.; Heinz, D. W.; Jahn, D. The substrate radical of *Escherichia coli* oxygen-independent coproporphyrinogen III oxidase HemN. *J. Biol. Chem.* **2006**, *281*, 15727−15734.
(21) Kuchenreuther, J. M.; Myers, W. K.; Stich, T. A.; George, S. J.; NejatyJahromy, Y.; Swartz, J. R.; Britt, R. D. A radical intermediate in tyrosine scission to the CO and CN^- ligands of FeFe hydrogenase. *Science* **2013**, *342*, 472−475.
(22) Frey, P. A.; Chang, C. H.; Ballinger, M. D.; Reed, G. H. Kinetic characterization of transient free radical intermediates in reaction of lysine 2,3-aminomutase by EPR lineshape analysis. *Methods Enzymol.* **2002**, *354*, 426−435.
(23) Brindley, A. A.; Zajicek, R.; Warren, M. J.; Ferguson, S. J.; Rigby, S. E. J. NirJ, a radical SAM family member of the d_1 heme biogenesis cluster. *FEBS Lett.* **2010**, *584*, 2461−2466.
(24) Zhang, Q.; Chen, D.; Lin, J.; Liao, R.; Tong, W.; Xu, Z.; Liu, W. Characterization of NocL involved in thiopeptide nocathiacin I biosynthesis. A 4Fe-4S cluster and the catalysis of a radical *S*-adenosylmethionine enzyme. *J. Biol. Chem.* **2011**, *286*, 21287−21294.
(25) Martinez-Gomez, N. C.; Poyner, R. R.; Mansoorabadi, S. O.; Reed, G. H.; Downs, D. M. Reaction of AdoMet with ThiC generates a backbone free radical. *Biochemistry* **2009**, *48*, 217−219.
(26) Cosper, M. M.; Jameson, G. N. L.; Davydov, R.; Eidsness, M. K.; Hoffman, B. M.; Huynh, B. H.; Johnson, M. K. The $[4Fe\text{-}4S]^{2+}$ cluster in reconstituted biotin synthase binds *S*-adenosyl-L-methionine. *J. Am. Chem. Soc.* **2002**, *124*, 14006−14007.
(27) Lanz, N. D.; Booker, S. J. Identification and function of auxiliary iron-sulfur clusters in radical SAM enzymes. *Biochim. Biophys. Acta* **2012**, *1824*, 1196−1212.
(28) Zhang, Q.; van der Donk, W. A.; Liu, W. Radical-mediated enzymatic methylation: A tale of two SAMS. *Acc. Chem. Res.* **2012**, *45*, 555−564.
(29) Magnusson, O. T.; Reed, G. H.; Frey, P. A. Spectroscopic evidence for the participation of an allylic analogue of the 5′-deoxyadenosyl radical in the reaction of lysine 2,3-aminomutase. *J. Am. Chem. Soc.* **1999**, *121*, 9764−9765.
(30) Magnusson, O. T.; Reed, G. H.; Frey, P. A. Characterization of an allylic analogue of the 5′-deoxyadenosyl radical: An intermediate in the reaction of lysine 2,3-aminomutase. *Biochemistry* **2001**, *40*, 7773−7782.
(31) Wang, S. C.; Frey, P. A. *S*-adenosylmethionine as an oxidant: the radical SAM superfamily. *Trends Biochem. Sci.* **2007**, *32*, 101−110.
(32) Ballinger, M. D.; Reed, G. H.; Frey, P. A. An organic radical in the lysine 2,3-aminomutase reaction. *Biochemistry* **1992**, *31*, 949−953.
(33) Wu, W. M.; Booker, S.; Lieder, K. W.; Bandarian, V.; Reed, G. H.; Frey, P. A. Lysine 2,3-aminomutase and trans-4,5-dehydrolysine: Characterization of an allylic analogue of a substrate-based radical in the catalytic mechanism? *Biochemistry* **2000**, *39*, 9561−9570.
(34) Lepore, B. W.; Ruzicka, F. J.; Frey, P. A.; Ringe, D. The X-ray crystal structure of lysine-2,3-aminomutase from *Clostridium subterminale*. *Proc. Natl. Acad. Sci. U.S.A.* **2005**, *102*, 13819−13824.
(35) Ballinger, M. D.; Frey, P. A.; Reed, G. H. Structure of a substrate radical intermediate in the reaction of lysine 2,3-aminomutase. *Biochemistry* **1992**, *31*, 10782−10789.
(36) Ballinger, M. D.; Frey, P. A.; Reed, G. H.; Lobrutto, R. Pulsed electron paramagnetic resonance studies of the lysine 2,3-aminomutase substrate radical-evidence for participation of pyridoxal 5′-phosphate in a radical rearrangement. *Biochemistry* **1995**, *34*, 10086−10093.
(37) Frey, P. A.; Reed, G. H. Pyridoxal-5′-phosphate as the catalyst for radical isomerization in reactions of PLP-dependent aminomutases. *Biochim. Biophys. Acta* **2011**, *1814*, 1548−1557.
(38) Lin, S.; Cronan, J. E. Closing in on complete pathways of biotin biosynthesis. *Mol. Biosyst.* **2011**, *7*, 1811−1821.
(39) Berkovitch, F.; Nicolet, Y.; Wan, J. T.; Jarrett, J. T.; Drennan, C. L. Crystal structure of biotin synthase, an S-adenosylmethionine-dependent radical enzyme. *Science* **2004**, *303*, 76−79.
(40) Fugate, C. J.; Jarrett, J. T. Biotin synthase: Insights into radical-mediated carbon-sulfur bond formation. *Biochim. Biophys. Acta* **2012**, *1824*, 1213−1222.
(41) This amounts to a modified version of eq 1 wherein the dipolar term is computed for the magnetic nucleus interacting with each spin center, the Fe(II) and Fe(III) ions in this case, and these values are then summed to give the net dipolar interaction.
(42) Randall, D. W.; Gelasco, A.; Caudle, M. T.; Pecoraro, V. L.; Britt, R. D. ESE-ENDOR and ESEEM characterization of water and methanol ligation to a dinuclear Mn(III)Mn(IV) complex. *J. Am. Chem. Soc.* **1997**, *119*, 4481−4491.
(43) Houseman, A. L. P.; Oh, B. H.; Kennedy, M. C.; Fan, C.; Werst, M. M.; Beinert, H.; Markley, J. L.; Hoffman, B. M. Nitrogen-14,15, carbon-13, iron-57, and proton−deuterium Q-band ENDOR study of iron−sulfur proteins with clusters that have endogenous sulfur ligands. *Biochemistry* **1992**, *31*, 2073−2080.
(44) Shepard, E. M.; Duffus, B. R.; George, S. J.; McGlynn, S. E.; Challand, M. R.; Swanson, K. D.; Roach, P. L.; Cramer, S. P.; Peters, J. W.; Broderick, J. B. FeFe-hydrogenase maturation: HydG-catalyzed synthesis of carbon monoxide. *J. Am. Chem. Soc.* **2010**, *132*, 9247−9249.
(45) Driesener, R. C.; Challand, M. R.; McGlynn, S. E.; Shepard, E. M.; Boyd, E. S.; Broderick, J. B.; Peters, J. W.; Roach, P. L. FeFe-hydrogenase cyanide ligands derived from *s*-adenosylmethionine-dependent cleavage of tyrosine. *Angew. Chem.* **2010**, *49*, 1687−1690.
(46) Kuchenreuther, J. M.; George, S. J.; Grady-Smith, C. S.; Cramer, S. P.; Swartz, J. R. Cell-free H-cluster synthesis and FeFe hydrogenase activation: All Five CO and CN^- ligands derive from tyrosine. *PLoS One* **2011**, *6*, No. e20346.
(47) Pilet, E.; Nicolet, Y.; Mathevon, C.; Douki, T.; Fontecilla-Camps, J. C.; Fontecave, M. The role of the maturase HydG in FeFe -hydrogenase active site synthesis and assembly. *FEBS Lett.* **2009**, *583*, 506−511.
(48) Decamps, L.; Philmus, B.; Benjdia, A.; White, R.; Begley, T. P.; Berteau, O. Biosynthesis of F_0, precursor of the F_{420} cofactor, requires a unique two radical-SAM domain enzyme and tyrosine as substrate. *J. Am. Chem. Soc.* **2012**, *134*, 18173−18176.
(49) Challand, M. R.; Martins, F. T.; Roach, P. L. Catalytic activity of the anaerobic tyrosine lyase required for thiamine biosynthesis in *Escherichia coli*. *J. Biol. Chem.* **2010**, *285*, 5240−5248.
(50) Kuchenreuther, J. M.; Myers, W. K.; Suess, D. L. M.; Stich, T. A.; Pelmenschikov, V.; Shiigi, S. A.; Cramer, S. P.; Swartz, J. R.; Britt, R. D.; George, S. J. The HydG enzyme generates an $Fe(CO)_2(CN)$ synthon in assembly of the FeFe hydrogenase H-cluster. *Science* **2014**, *343*, 424−427.
(51) Wagner, A. F. V.; Frey, M.; Neugebauer, F. A.; Schafer, W.; Knappe, J. The free radical in pyruvate formate lyase is located on glycine-734. *Proc. Natl. Acad. Sci. U.S.A.* **1992**, *89*, 996−1000.
(52) Hulsebosch, R. J.; vandenBrink, J. S.; Nieuwenhuis, S. A. M.; Gast, P.; Raap, J.; Lugtenburg, J.; Hoff, A. J. Electronic structure of the neutral tyrosine radical in frozen solution. Selective H-2-, C-13-, and O-17-isotope labeling and EPR spectroscopy at 9 and 35 GHz. *J. Am. Chem. Soc.* **1997**, *119*, 8685−8694.
(53) Hanzelmann, P.; Schindelin, H. Binding of 5′-GTP to the C-terminal FeS cluster of the radical S-adenosylmethionine enzyme MoaA provides insights into its mechanism. *Proc. Natl. Acad. Sci. U.S.A.* **2006**, *103*, 6829−6834.
(54) Lees, N. S.; Hanzelmann, P.; Hernandez, H. L.; Subramanian, S.; Schindelin, H.; Johnson, M. K.; Hoffman, B. M. ENDOR spectroscopy shows that guanine N1 binds to 4Fe-4S cluster II of the *S*-adenosylmethionine-dependent enzyme MoaA: Mechanistic implications. *J. Am. Chem. Soc.* **2009**, *131*, 9184−9185.
(55) Yan, F.; LaMarre, J. M.; Roehrich, R.; Wiesner, J.; Jomaa, H.; Mankin, A. S.; Fujimori, D. G. RlmN and Cfr are radical SAM enzymes involved in methylation of ribosomal RNA. *J. Am. Chem. Soc.* **2010**, *132*, 3953−3964.
(56) Boal, A. K.; Grove, T. L.; McLaughlin, M. I.; Yennawar, N. H.; Booker, S. J.; Rosenzweig, A. C. Structural basis for methyl transfer by a radical SAM enzyme. *Science* **2011**, *332*, 1089−1092.
(57) Sofia, H. J.; Chen, G.; Hetzler, B. G.; Reyes-Spindola, J. F.; Miller, N. E. Radical SAM, a novel protein superfamily linking unresolved steps in familiar biosynthetic pathways with radical

mechanisms: Functional characterization using new analysis and information visualization methods. *Nucleic Acids Res.* **2001**, *29*, 1097−1106.
(58) http://sfld.rbvi.ucsf.edu/django/superfamily/29/.
(59) Buckel, W.; Friedrich, P.; Golding, B. T. Hydrogen bonds guide the short-lived 5′-deoxyadenosyl radical to the place of action. *Angew. Chem., Int. Ed.* **2012**, *51*, 9974−9976.
(60) Dowling, D. P.; Vey, J. L.; Croft, A. K.; Drennan, C. L. Structural diversity in the AdoMet radical enzyme superfamily. *Biochim. Biophys. Acta* **2012**, *1824*, 1178−1195.